International Journal of Engineering

New Dominant Color Descriptor Features Based on Weighting of More Informative Pixels using Suitable Masks for Content-Based Image Retrieval

S. Fadaei*

Department of Electrical Engineering, Faculty of Engineering, Yasouj University, Yasouj, Iran

A B S T R A C T

Content-based image retrieval (CBIR) is a process of retrieving images based on their content in a dataset automatically. CBIR is a common solution to search images similar to a desired image among all images in dataset. To do this, many methods have been developed to extract images features. Here, a new Dominant Color Descriptor (DCD) method is proposed to improve CBIR accuracy. In the first step, Canny edges of images are extracted. In the next step, edges are widened by employing morphological operations. Finally, pixels that are not at the edges are weighted less than the pixels which are located at edges. Indeed, pixels in regions with low color variations are less weighted and more informative pixels are more weighted in providing DCD features. To show the effectiveness of the proposed method, experiments are performed on three datasets Corel-1k, Corel-10k and Caltech256. Results demonstrate that the proposed method outperforms competitive methods.

doi: 10.5829/ije.2022.35.08b.01

1. INTRODUCTION

Due to mobile phones, digital cameras and other digital imaging equipments, image libraries have been greatly enlarged and managing these images is very tedious and, in some cases, is impossible for humans to handle. So, an automatic technique to search for a desired image from the huge dataset is necessary. Content-based image retrieval (CBIR) is a common solution for this problem. In CBIR, images are mapped to a feature vector and then retrieval process is done. It is tried to make feature vector containing a lot of information of the image. In the retrieval step, the feature vector of desired image (query) is compared with images in dataset and images with less distance to query are retrieved. The feature extraction is a vital step in CBIR and affects retrieval accuracy is significant [1, 2].

Color, texture and shape are the most important features of images. Among these features, color features are the most significant features which are robust agaist object rotation and translation [3]. Singha et al. [4] have used histogram as a color feature in images. A new method based on color coherence vector (CCV) was proposed by Pass and Zabih [5]. Similar to color histogram method, CCV is computed from color histogram by considering bins as incoherent or coherent. Chun et al. [6] have used color auto-correlograms of H and S components in HSV domain as color discriptors and combined with texture components as feature vector. DCD is another feature extraction method in which the image color space is partitioned into limited number of partitions [7].

Talib et al. [8] presented a new semantic feature extraction method named as weighted DCD in which each dominant color is weighted properly. The weighted DCD method diminishes the bad effect of backgrounds in images and highlights the foreground or object. To do this, three different weights Borther Weight of Dominant

*Corresponding Author Institutional Email: s.fadaei@yu.ac.ir (S. Fadaei)

Color (BWDC), Salient Object Weights (SOW) and Dominant Color Weights (DCW) are introduced and final dominant color weights are calculated using these weights. Also, a similarity measure based on Mutual Color Ratio (MCR) is modified to consider the defined weights. A new CBIR method by optimize combination of color and texture features is introduced by Fadaei et al. [9] to increase CBIR retrieval accuracy. A fast color quantization method with clusters merging is presented by Deng et al. [10] to achieve effective color features. Then some texture and shape features added to color features to increase the precision of CBIR system.

Wang et al. [11] proposed an efficient and compact color descriptor as well as a convenient similarity measure similar to the quadratic color histogram distance. As the original quadratic histogram similarity measure does not work well for DCDs in MPEG-7, a measure of similiraty between histograms is used by Po and Wong [12] to address drawbacks of quadratic histogram similarity measure. Mojsilovic et al. [13] obtained DCD features in Lab color space and a new similarity measure was defined to address the issue of how humans measure the similarity of images within the color domain. Speed of CBIR is improved by Fadaei and Rashno [14] based on integration of Zernike and wavelet components by PSO.

Drawbacks of DCD were addressed by Pavithra and Sharmila [1] while considereding first, middle and last points of values in color interval. Another efficient seed point selection method was presented by Pavithra and Sharmila [15] to drawbacks of DCD. Xie et al. [16] used the texton template to extract consistent area of the image and then DCD features are extracted from the pixels of the consistent area. By employing Convlutional Neural Network by Sezavar et al. [17], CBIR was implemented based on high-level features to increase the CBIR precision.

DCD provides compact and precise features and is easy and fast in implementation. In this research we focussed on these features and improved them to increase the CBIR precision. As mentioned before, statistical parameters of similar color clusters were considered as DCD features. It is obvious that the number of pixels in different partitions is not equal and for some partitions is high while it is very low for another. On the other hand, there are important and fundamental information of an image in its edges while regions of less color variations have no significant information. Therefore, here, a new procedure is proposed to assign low weight to pixels in regions with low color variations and emphasize on pixels placed on edges and their neighbors. To do this, edges of image are detected firstly and then edges width is widened. Finally, pixels that are on edges are weighted more than the pixels not located on edges.

The remained sections are organized as follows: The proposed method is presented in section 2. Experimental setup and results are reported in sections 3 and 4 and the paper is concluded in section 5.

2. PROPOSED DCD FEATURES

2. 1. DCD Feature Extraction Method
DCD features have been widely used in previous researches because extracting of them is easier and faster than the other features. Providing a compact description of the color distribution of the image is another advantage of these features. As shown in Figure 1, the color space is firstly divided into several partitions in the DCD method. Each pixel of the image belongs to a partition. The mean color of the pixels and percentage of them in each partition are used as DCD features.

It is clear from Figure 2 that partitions 2 (Figure 2c), 4 (Figure 2e) and 6 (Figure 2g) have few pixles, so it is expected that the corresponding percentage of these partitions should be low. According to Figure 2k, the percentage of these partitions are 0.00048, 0.00014 and 0.00150, respectively.

2. 2. Proposed Method
As mentioned before, pixels located on edges and their neighbors are more informative than the other pixels and in contrast, regions with less color variations have no significant information. If the number of pixels located in several partitions of the color space is very different, then the extracted DCD features will not perform well. To address this drawback, weighted DCD was proposed by Talib et al. [8] in which lower weights are assigned to the background section and higher weights are assigned to the object. Although it was tried to solve this problem in weighted DCD, but the weights have not been properly adjusted and does not work well.

To address this challenge, a new method is proposed here. The proposed method is inspired by this property that edeges contain significant information of images. Indeed, the colors of the edge pixels are given higher weight in the proposed method and pixels in regions with low color variations are given lower weight. Therefore, the edges of the image should be segmented and used to form DCD features.
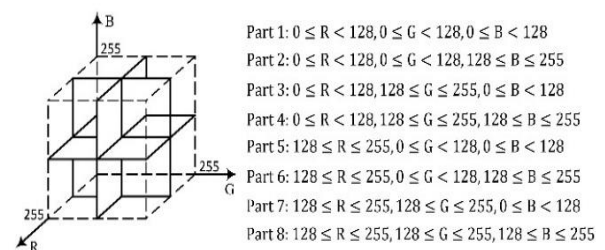

Figure 1. Dividing RGB into 8 partitions in DCD method

	R	G	B
C1	74.9	76.7	51.9
C2	124.1	120.7	131.0
C3	114.5	139.2	76.5
C4	125.2	133.9	131.4
C5	142.4	115.8	76.3
C6	134.8	123.5	133.7
C7	158.3	149.6	93.7
C8	214.3	212.3	213.1

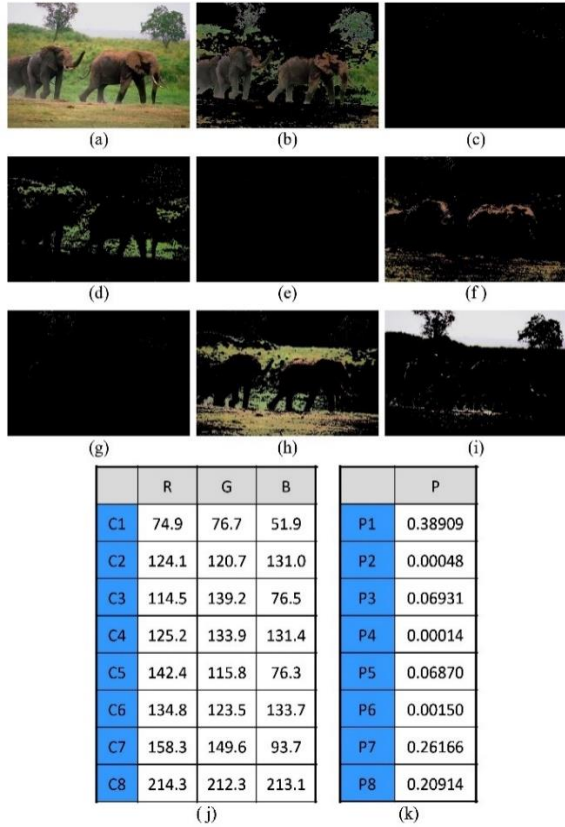|	P
P1	0.38909
P2	0.00048
P3	0.06931
P4	0.00014
P5	0.06870
P6	0.00150
P7	0.26166
P8	0.20914

(j)   (k)

Figure 2. Implementation of DCD method on a sample image of the Corel-1k dataset; a) the original image, b-i) the pixels belonging to partitions 1 to 8, j) mean of pixels in each partition and k) percentage of pixels in each partition

Figure 3 illustrates the diagram of the proposed method. In this method, at first, the input image is transferred to gray-level domain and then the edges of the image are extracted. Since the edges of the image contain a lot of information, the purpose of this stage is to extract edges locations. The pixels around the edges also contain high color information, so, the morphological dilation is applied to edge image to widen the edges. According to Figure 3, location of the edges and their neighbors are determined in this step.

Output of this step is two binary images: The first image is 1 in locations with important information (edges and their neighbors) and is 0 in the others. The second image is the opposite of first image so that is 0 in edge locations and 1 in the others. In the next step, the binary images are used as mask and multiplied by the input image. Finally, two images are obtained which the DCD features are extracted from these images by suitable weighting.

The input image is shown by I with size $X \times Y$ and the color information of pixel (x, y) is indicated by $I(x, y)$. At first, the input image is transferred to gray-level domain:

$$G(x,y) = \frac{I_R(x,y) + I_G(x,y) + I_B(x,y)}{3} \qquad (1)$$

where $I_R(x, y)$, $I_G(x, y)$ and $I_B(x, y)$ are red, green and blue components of the image and $G(x, y)$ is the gray-scale image. Edges of the gray image $G(x, y)$ are extracted using Canny edge detector in the next step. The edge image is indicated by $G_E(x, y)$ and is 1 on edge locations and 0 on the others.

In the next step, edge image is dilated by a disk-shaped structuring element with diameter D. The disk-shaped structuring element is indicated by S_D and the edges are thickened in proportion to the D:

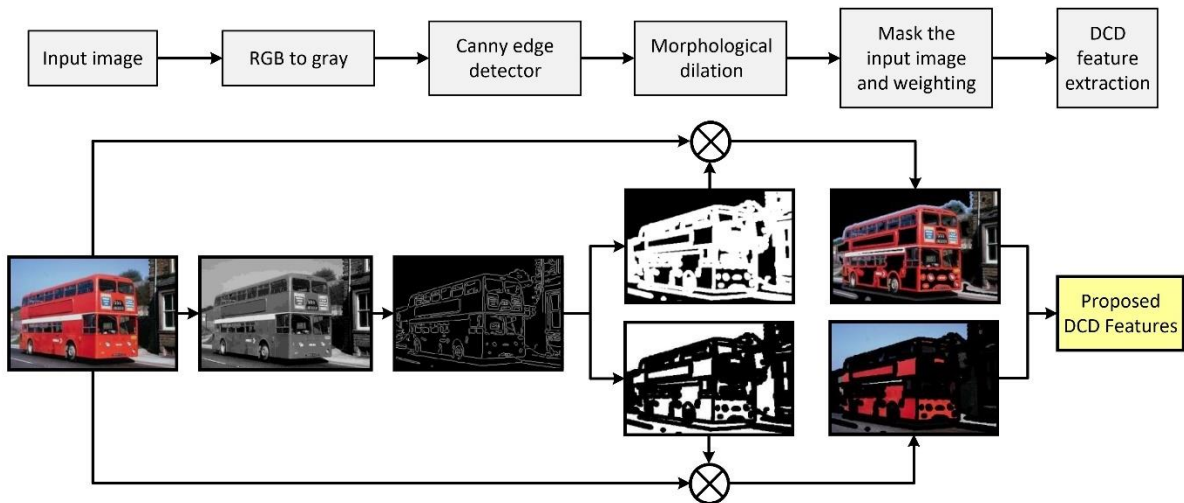$$M_{H,D} = G_E \oplus S_D = \{z | (\hat{S}_D)_z \cap G_E \neq \phi\} \qquad (2)$$

Figure 3. Flowchart of the proposed method

where $\oplus$ is dilation operator, $\hat{S}_D$ indicates the complement of S_D, $(\hat{S}_D)_z$ is the translation of $\hat{S}_D$ by z and $M_{H,D}$ is a binary image which is 1 on edges and their neighbors and 0 on other locations. Therefore $M_{H,D}$ is a mask that can be used to determine the pixels located at the edges which contain a lot of information. Based on mask $M_{H,D}$, mask $M_{L,D}$ is defined which is 1 in regions with low variations and 0 in other locations.

$$M_{L,D} = 1 - M_{H,D} \tag{3}$$

In the next step, the pixels with more and less information are determined:

$$I_{H,D}(x,y) = M_{H,D}(x,y) \times I(x,y) \tag{4}$$

$$I_{L,D}(x,y) = M_{L,D}(x,y) \times I(x,y) \tag{5}$$

In DCD method, the color space is partitioned to N partitions and pixels that are placed in each partition are identified. To do this, a mask is defined for each partition as follows:

$$M_{P,i}(x,y) = \begin{cases} 1, & \alpha_{a,i} \leq I_R(x,y) < \alpha_{b,i} \text{ and} \\ & \beta_{a,i} \leq I_G(x,y) < \beta_{b,i} \text{ and} \\ & \gamma_{a,i} \leq I_B(x,y) < \gamma_{b,i} \\ 0, & \text{otherwise} \end{cases} \tag{6}$$

Where $M_{P,i}$ is the mask of ith partition and is 1 for pixels belong to that partition and 0 for the others. $\alpha_{a,i}$ and $\alpha_{b,i}$ are the low and high limit of the ith partition for the first component of color space, $\beta_{a,i}$ and $\beta_{b,i}$ are the low and high limits of the second component of partition i in color space and $\gamma_{a,i}$ and $\gamma_{b,i}$ are the low and high limits for the third component. In the next step the center and percentage of each partition is calculated as follows:

$$C_{R,i} = \frac{1}{|M_{P,i}|}\sum_{y=1}^{Y}\sum_{x=1}^{X} M_{P,i}(x,y) \times \left(k_H I_{H,D}^R(x,y) + k_L I_{L,D}^R(x,y)\right) = \frac{1}{|M_{P,i}|}\sum_{y=1}^{Y}\sum_{x=1}^{X} M_{P,i}(x,y) \times \left[k_H M_{H,D}(x,y) \times I_R(x,y) + k_L M_{L,D}(x,y) \times I_R(x,y)\right] \tag{7}$$

$$C_{G,i} = \frac{1}{|M_{P,i}|}\sum_{y=1}^{Y}\sum_{x=1}^{X} M_{P,i}(x,y) \times \left(k_H I_{H,D}^G(x,y) + k_L I_{L,D}^G(x,y)\right) = \frac{1}{|M_{P,i}|}\sum_{y=1}^{Y}\sum_{x=1}^{X} M_{P,i}(x,y) \times \left[k_H M_{H,D}(x,y) \times I_G(x,y) + k_L M_{L,D}(x,y) \times I_G(x,y)\right] \tag{8}$$

$$C_{B,i} = \frac{1}{|M_{P,i}|}\sum_{y=1}^{Y}\sum_{x=1}^{X} M_{P,i}(x,y) \times \left(k_H I_{H,D}^B(x,y) + k_L I_{L,D}^B(x,y)\right) = \frac{1}{|M_{P,i}|}\sum_{y=1}^{Y}\sum_{x=1}^{X} M_{P,i}(x,y) \times \left[k_H M_{H,D}(x,y) \times I_B(x,y) + k_L M_{L,D}(x,y) \times I_B(x,y)\right] \tag{9}$$

$$P_i = \frac{|M_{P,i}|}{X \times Y} \tag{10}$$

where k_H and k_L are assigned weights to more and less important pixels, respectively, and $|M_{P,i}|$ is defined as follows:

$$|M_{P,i}| = \sum_{y=1}^{Y}\sum_{x=1}^{X} M_{P,i}(x,y) \tag{11}$$

Finally, the proposed feature vector is formed by Equation (12), which is a vector of length $4N$:

$$F = \{C_{R,1}, C_{G,1}, C_{B,1}, P_1, \dots, C_{R,N}, C_{G,N}, C_{B,N}, P_N\} \tag{12}$$

2. 3. Distance Measure   Each CBIR system is working based on distance between query image and images in dataset. Since distance computation method proposed by Mojsilovic et al. [13] is used in this research, it is described in details as follows:

Suppose that images Q and DB are query and an image of dataset and their feature vectors are:

$$F_Q = \{(C_a^Q, P_a^Q), a = 1,2, \dots, N_Q\} \tag{13}$$

$$F_{DB} = \{(C_b^{DB}, P_b^{DB}), b = 1,2, \dots, N_{DB}\} \tag{14}$$

where, C and P are the dominant color and its percentage, respectively. At first, distance between Q and DB with respect to ith dominant color of image Q is defined as:

$$D(Q_i, DB) = \min_{b \in [1, N_{DB}]} d\left((C_i^Q, P_i^Q), (C_b^{DB}, P_b^{DB})\right) \tag{15}$$

$$d\left((C_i^Q, P_i^Q), (C_b^{DB}, P_b^{DB})\right) = |P_i^Q - P_b^{DB}| + \sqrt{\sum_{k=1}^{3}(C_{i,k}^Q - C_{b,k}^{DB})^2} \tag{16}$$

where, $C_{i,k}^Q$ is the kth component of dominant color C_i^Q. In the next step, $D(Q_i, DB)$ and $D(DB_i, Q)$ are calculated for $i = 1,2, \dots N_Q$ and $i = 1,2, \dots N_{DB}$, respectively. Finally, distanse between two images Q and DB is defined as follows:

$$Distance(Q, DB) = \sum_{a=1}^{N_{DB}} D(Q_i, DB) + \sum_{a=1}^{N_Q} D(DB_i, Q) \tag{17}$$

3. EXPERIMENTAL SETUP

3. 1. Datasets   Three datasets including Corel-1k, Corel-10k and Caltech256 are used for evaluation. As reported in Table 1, Corel-1k dataset consists of 10 classes, 100 images in each class and total number of images is 1000; Corel-10k consists of 100 classes, 100 images per class and total number of images is 10000; Caltech256 consists of 257 classes and 30607 images.

3. 2. Performance Evaluation Criteria   Precision, Recall, P10, Average Retrieval Rate (ARR), Average Normalized Modified Retrieval Rank (ANMRR) and Mean Average Precision (MAP) are used as evaluation criteria.

TABLE 1. Details of datasets Corel-1k, Corel-10k and Caltech256

Dataset	Classes	Total images	Images per class		
			min	max	mean
Corel-1k	10	1000	100	100	100
Corel-10k	100	10000	100	100	100
Caltech256	257	30607	80	827	119

To obtain precision, one image of the dataset images is considered as query image. Then, the feature vectors are extracted for query image and all images in dataset. In the next step, the distance between the query image and other images in dataset are obtained using Equation (17). Finally, the first T images in dataset with the lower distance from the query image are considered as images similar to the query. From these T images, some of them (suppose N) are from the class of query image and the rest are not. Therefore, the precision and recall of this experiment are:

$$P = \frac{N}{T} = \frac{\text{Number of similar images retrieved}}{\text{Total number of images retrieved}} \quad (18)$$

Recall is defined as:

$$R = \frac{N}{K} = \frac{\text{Number of similar images retrieved}}{\text{Total number of similar images in dataset}} \quad (19)$$

where N, T and K are number of similar retrived images, total number of retrieved images, and total number of similar images in dataset, respectively.

P10 is the average precision of 10 retrieved images. Indeed, P10 is the precision for $T = 10$.

ARR is calculated as follows:

$$ARR = \frac{1}{N_q} \sum_{q=1}^{N_q} RR_q \quad (20)$$

where, N_q is the number of query images used in the test which is set to all images in the dataset (E.g. $N_q = 1000$ for Corel-1k) and RR_q is calculated as follows:

$$RR_q = \frac{NR_q(\alpha)}{NG_q} \quad (21)$$

NG_q is the total number of relevant images with query q in the dataset and $NR_q(\alpha)$ is the number of relevant images retrieved in the first αNG_q. Here, α is configured to 1.

ANMRR is introduced as follows:

$$ANMRR = \frac{1}{N_q} \sum_{q=1}^{N_q} NMRR_q \quad (22)$$

$$NMRR_q = \frac{2 \times AVR_q - NG_q - 1}{2 \times W_q - NG_q + 1} \quad (23)$$

$$AVR_q = \frac{1}{NG_q} \sum_{i=1}^{NG_q} Rank_i \quad (24)$$

where, $W_q = 2NG_q$ and $Rank_i$ is calculated as follows: W images are retrieved for query q. Then, the ith relevant image to the query q is considered, if it is among these W images the $Rank_i$ is adjusted according to the order of this image in the W retrieved images, otherwise, it set to $W + 1$. Note that the best and worst values of ANMRR are 0 and 1, respectively. Indeed, the lower value of ANMRR is equivalent with the higher retrieval performance.

MAP is calculated as follows:

$$MAP = \frac{1}{N_q} \sum_{q=1}^{N_q} AP_q \quad (25)$$

$$AP_q = \frac{1}{NG_q} \sum_{i=1}^{NG_q} P_i \quad (26)$$

To calculate P_i, the order of ith relevant image in the retrieved images is considered as the number of retrieved images and the precision is calculated as P_i. It is worth mentioning that MAP measures the retrieval precision among all relevant images in the dataset while ANMRR calculates the precision for a window W.

4. EXPERIMENTAL RESULTS

4. 1. Structuring Element Impact   In the first experiment, the impact of SE size of morphological dilation on these datasets is evaluated. The structuring element is a disk. Here, the precision is considered for evaluation and $T = 20$. To obtain the precision for each SE size, precision of all images in dataset is calculated and then, the final precision is averaged over all precisions. Therefore, the reported values on the Corel-1k, Corel-10k and Caltech256 datasets are averaged over 1000, 10000 and 30607 experiments, respectively. Figure 4 shows precision of these datasets for different SE size. The Corel-1k dataset for SE size of 47 has achieved a maximum precision of 70.87% and the maximum precision in Corel-10k and Caltech256 datasets are 40.75% and 11.65%, respectively, for SE size of 25 and 15.

4. 2. Impact of Retrieved Images Number Number of retrieved images is varied from 5 to 40 and the precision and recall are calculated for each dataset in the best SE size. Precision and recall results are reported in Table 2, Figures 5 and 6 for Corel-1k, Corel-10k and Caltech256 datasets.

Based on Figure 5, precision is decreased by increment of retrieved images.

As the number of retrieved images increases, the recall increases which can be seen in Figure 6.

4. 3. Comparing the Proposed Method with Other Methods   In this experiment, the precision and
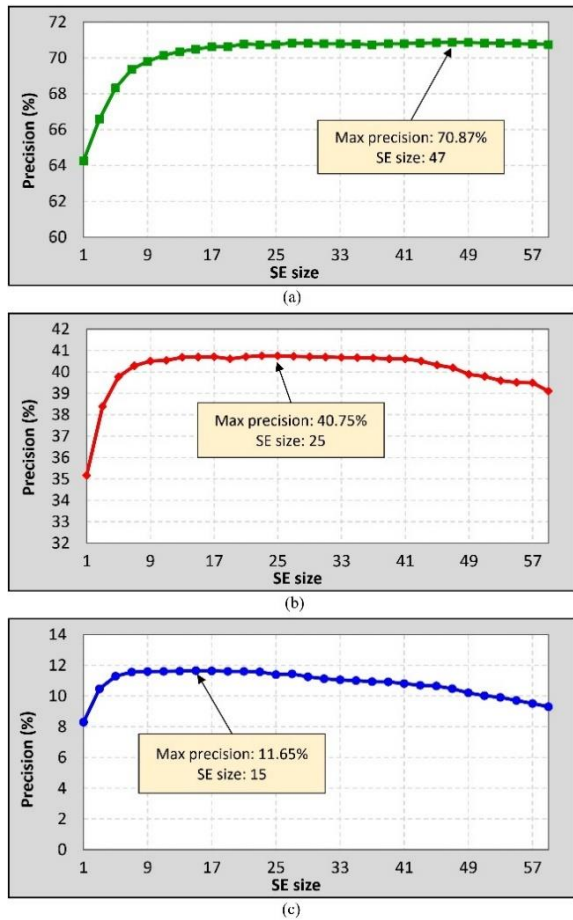
Figure 4. Precision results for SE size in a) Corel-1k, b) Corel-10k and c) Caltech256 datasets

TABLE 2. Precision and recall results of the proposed method for different number of retrieved images in Corel-1k, Corel-10k and Caltech256 datasets

T	Precision (%)			Recall (%)		
	Corel-1k	Corel-10k	Caltech256	Corel-1k	Corel-10k	Caltech256
5	83.28	61.35	27.06	4.16	3.07	1.14
10	77.15	50.06	16.61	7.72	5.01	1.40
15	73.66	44.37	12.94	11.05	6.66	1.63
20	70.87	40.75	11.65	14.17	8.15	1.96
25	68.57	37.94	9.85	17.14	9.49	2.07
30	66.59	35.70	9.02	19.98	10.71	2.27
35	64.79	33.85	8.42	22.68	11.85	2.48
40	63.13	32.25	7.95	25.25	12.90	2.67

recall of the proposed scheme are compared with previous methods on the Corel-1k, Corel-10k and Caltech256. Precision and recall of the proposed method

and literature [8, 10-13,15] in Corel-1k dataset are shown in Tables 3 and 4. Figure 7 demonstrates the precision of the proposed method and other methods. In this experiment number of retrieved images is configured to $T = 20$.
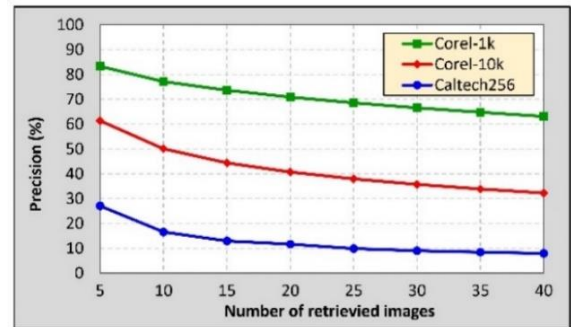

Figure 5. Precision results for different number of retrieved images (T) in Corel-1k, Corel-10k and Caltech256 datasets
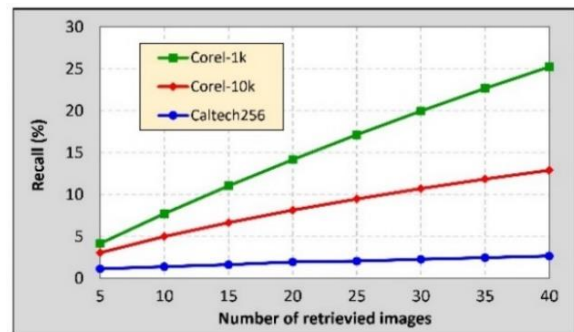

Figure 6. Recall results for different number of retrieved images (T) in Corel-1k, Corel-10k and Caltech256 datasets

TABLE 3. Precision of the proposed method and literature [8, 10-13,15] in Corel-1k dataset.

Class	Precision (%)						
	[11]	[8]	[10]	[12]	[13]	[15]	Proposed
Africa	53.50	51.25	58.35	64.10	65.65	69.27	**72.05**
Beach	39.50	39.60	41.35	43.10	44.65	**45.12**	36.85
Building	38.10	44.25	39.85	45.85	52.35	44.31	**74.00**
Bus	46.70	47.75	61.10	53.70	65.00	71.46	**77.10**
Dinosaur	99.70	79.45	99.25	99.95	**100.00**	96.36	97.20
Elephant	51.15	54.55	55.40	53.60	53.85	55.10	**58.20**
Flower	53.95	63.35	67.90	70.00	**94.40**	81.05	84.65
Horse	81.45	83.40	**94.05**	90.95	89.50	79.61	90.75
Mountain	30.35	36.60	32.80	39.50	44.10	**45.83**	43.10
Food	58.50	61.95	59.95	67.00	68.95	72.43	**74.80**
Win	**0**	**0**	**1**	**0**	**2**	**2**	**5**

TABLE 4. Recall of the proposed method and literature [8, 10-13, 15] in Corel-1k dataset

Class	Recall (%)						
	[11]	**[8]**	**[10]**	**[12]**	**[13]**	**[15]**	**Proposed**
Africa	10.70	10.25	11.67	12.82	13.13	13.85	**14.41**
Beach	7.90	7.92	8.27	8.62	8.93	**9.02**	7.37
Building	7.62	8.85	7.97	9.17	10.47	8.86	**14.80**
Bus	9.34	9.55	12.22	10.74	13.00	14.29	**15.42**
Dinosaur	19.94	15.89	19.85	19.99	**20.00**	19.27	19.44
Elephant	10.23	10.91	11.08	10.72	10.77	11.02	**11.64**
Flower	10.79	12.67	13.58	14.00	**18.88**	16.21	16.93
Horse	16.29	16.68	**18.81**	18.19	17.90	15.92	18.15
Mountain	6.07	7.32	6.56	7.90	8.82	**9.17**	8.62
Food	11.70	12.39	11.99	13.40	13.79	14.49	**14.96**
Win	**0**	**0**	**1**	**0**	**2**	**2**	**5**
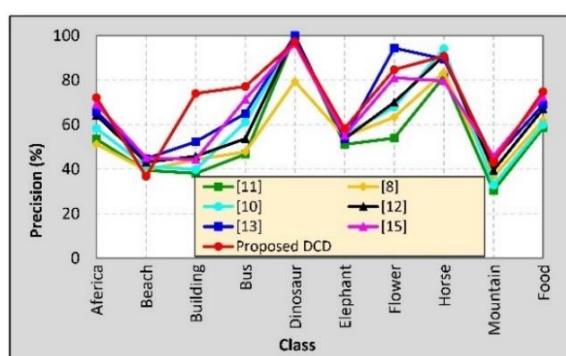
Figure 7. Precision of the proposed method and literature [8, 10-13,15] in Corel-1k dataset

Tables 3 and 4 indicate that the proposed method makes superior precision results in comparison with competetive methods in 5 classes out of 10 classes.

Table 5 and Figure 8 indicates the average precision over all classes in Corel-1k, Corel-10k and Caltech256 for all methods. It may be concluded that: 1) The proposed method outperforms literature [8, 10-13,15] by 14.66%, 9.87%, 15.58%, 8.10%, 3.02% and 4.82% with respect to average precision in Corel-1k; 2) The proposed method works better than [11] by 16.73%, [8] by 14.00%, [10] by 15.43%, [12] by 11.97%, [13] by 7.03% and [15] by 7.83% in terms of average precision in Corel-10k; 3) Although method by Mojsilovic et al. [13] has reached precision of 11.87% in Caltech256 and is the best method in this dataset, but the proposed method with precision 11.65% is very close to this method.

In the next experiment, to compare the proposed method with the other methods, the metrics P10, ARR, ANMRR and MAP for Corel-1k are considered. Tables

TABLE 5. Precision of the proposed method and literature [8, 10-13, 15] in three datasets Corel-1k, Corel-10k and Caltech256

Dataset	Precision (%)						
	[11]	**[8]**	**[10]**	**[12]**	**[13]**	**[15]**	**Proposed**
Corel-1k	55.29	56.21	61.00	62.77	67.85	66.05	**70.87**
Corel-10k	24.02	26.75	25.32	28.78	33.72	32.92	**40.75**
Caltech256	8.87	8.71	7.91	10.27	**11.87**	11.06	11.65
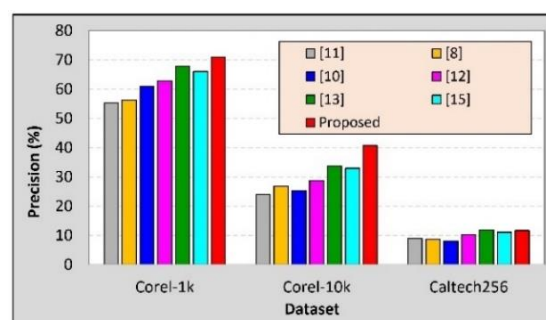
Figure 8. Precision of the proposed method and literature [8, 10-13,15] in three datasets Corel-1k, Corel-10k and Caltech256

6-9 report the P10, ARR, ANMRR and MAP of the proposed method and methods in literature [8, 10-13,15] on Corel-1k dataset.

It cab be concluded from Tables 6-9 that: 1) The proposed method outperforms methods in literature [8, 10-13, 15] in terms of P10, ARR, ANMRR and MAP; 2). The proposed method is the best method in 5, 4, 4 and 5 classes out of 10 classes in P10, ARR, ANMRR and MAP measures, respectively.

TABLE 6. P10 of the proposed method and literature [8, 10-13,15] in Corel-1k dataset.

Class	Method						
	[11]	**[8]**	**[10]**	**[12]**	**[13]**	**[15]**	**Proposed**
Africa	0.5910	0.4930	0.6446	0.7190	0.7120	0.7652	**0.7940**
Beach	0.4520	0.4360	0.4732	0.5960	0.3870	**0.5163**	0.4400
Building	0.4560	0.6220	0.4769	0.5330	0.7320	0.5303	**0.8070**
Bus	0.5270	0.4530	0.6895	0.5980	0.7000	0.7664	**0.8110**
Dinosaur	**0.9970**	0.8860	0.9925	0.9960	0.8400	0.9636	0.9930
Elephant	0.6190	0.5160	0.6804	0.6560	0.6340	0.6767	**0.7100**
Flower	0.6040	0.7040	0.7502	0.8410	**0.9140**	0.8955	0.9000
Horse	0.8760	0.9050	**1.0000**	0.8230	0.9860	0.8465	0.9600
Mountain	0.3620	0.4270	0.3782	0.4640	0.5160	**0.5285**	0.5040
Food	0.6610	0.6920	0.6774	0.6770	0.7910	0.7884	**0.7960**
Average	0.6145	0.6134	0.6763	0.6903	0.7212	0.7277	**0.7715**

TABLE 7. ARR of the proposed method and literature [8, 10-13, 15] in Corel-1k dataset

Class	Method						
	[11]	[8]	[10]	[12]	[13]	[15]	Proposed
Africa	0.3757	0.3328	0.4351	0.4171	0.3848	**0.5166**	0.4133
Beach	0.2649	0.2592	0.2813	0.3112	0.2584	**0.3169**	0.2343
Building	0.2536	0.3333	0.2556	0.2443	0.4520	0.3342	**0.5041**
Bus	0.3551	0.3271	0.4679	0.3359	0.4077	0.5001	**0.5022**
Dinosaur	0.9785	0.4291	0.4807	0.9815	0.5102	0.4867	**0.7566**
Elephant	0.3469	0.3525	**0.4948**	0.3576	0.3634	0.4922	0.3399
Flower	0.3143	0.3741	0.3786	0.4642	0.4095	0.4820	**0.6401**
Horse	0.4555	0.4299	0.4750	0.3919	**0.6522**	0.4321	0.5897
Mountain	0.2221	0.2648	0.2346	0.2202	**0.3590**	0.3277	0.2758
Food	0.3741	0.4017	0.4132	0.3483	**0.5434**	0.4809	0.4792
Average	0.3941	0.3505	0.3917	0.4072	0.4341	0.4369	**0.4735**

TABLE 8. ANMRR of the proposed method and literature [8, 10-13, 15] in Corel-1k dataset

Class	Method						
	[11]	[8]	[10]	[12]	[13]	[15]	Proposed
Africa	0.5416	0.5853	0.5207	0.5081	0.5390	0.6512	**0.5000**
Beach	0.6630	0.6673	0.6541	0.6272	0.6844	**0.5231**	0.7067
Building	0.6760	0.5815	0.6870	0.6829	0.4449	0.3884	**0.3839**
Bus	0.5527	0.5802	0.6731	0.5858	0.5158	0.7041	**0.4013**
Dinosaur	**0.0102**	0.4902	0.0302	0.0952	0.3873	0.2962	0.1422
Elephant	0.5662	0.5613	0.6024	0.5645	**0.5535**	0.5733	0.5735
Flower	0.6356	0.5504	0.7194	0.4590	0.5188	0.4148	**0.2663**
Horse	0.4549	0.4785	0.4393	0.5332	**0.2463**	0.4565	0.3110
Mountain	0.7124	0.6629	0.6044	0.7132	0.5618	**0.5468**	0.6503
Food	0.5278	0.5026	0.5109	0.5890	**0.3607**	0.5773	0.4192
Average	0.5340	0.5660	0.5441	0.5358	0.4812	0.4714	**0.4354**

TABLE 9. MAP of the proposed method and literature [8, 10-13, 15] in Corel-1k dataset

Class	Method						
	[11]	[8]	[10]	[12]	[13]	[15]	Proposed
Africa	0.3683	0.3180	0.4357	0.3819	0.4383	**0.5285**	0.4372
Beach	0.2753	0.2609	0.2831	0.3275	**0.3453**	0.3440	0.2236
Building	0.2488	0.3305	0.3034	0.2796	0.3188	0.3668	**0.5446**
Bus	0.3459	0.3223	0.4811	0.3642	0.4725	0.5304	**0.5447**
Dinosaur	0.9866	0.4689	0.5752	0.9906	**1.0000**	0.5449	0.8335
Elephant	0.3379	0.3375	0.4737	0.3754	0.4079	**0.4776**	0.3506
Flower	0.2946	0.3780	0.3825	0.4914	0.3646	0.5157	**0.6956**
Horse	0.4717	0.4704	0.5198	0.4027	0.5417	0.4750	**0.6398**
Mountain	0.2049	0.2554	0.2263	0.2597	0.2749	**0.3611**	0.2751
Food	0.3937	0.4284	0.4407	0.3141	0.4637	0.5130	**0.5188**
Average	0.3928	0.3570	0.4122	0.4187	0.4628	0.4657	**0.5064**

TABLE 10. Precision of the proposed method and literature [18-25] in Corel-1k dataset

Class	Precision (%)								
	[18]	[19]	[20]	[21]	[22]	[23]	[24]	[25]	Proposed
Africa	83.00	77.82	69.08	73.03	72.50	51.00	64.00	83.00	**99.40**
Beach	72.00	79.56	72.20	74.58	65.20	**90.00**	54.00	82.85	60.60
Building	86.00	80.75	84.85	80.24	70.60	58.00	53.00	82.00	**97.00**
Bus	**100.0**	95.74	95.75	95.84	89.20	78.00	94.00	**100.0**	99.80
Dinosaur	97.00	98.12	**100.0**	97.95	**100.0**	**100.0**	98.00	**100.0**	**100.0**
Elephant	82.00	89.54	89.99	87.64	70.50	84.00	78.00	**90.00**	88.00
Flower	86.00	86.87	94.01	85.13	94.80	**100.0**	71.00	95.00	**100.0**
Horse	82.00	89.41	86.38	86.29	91.80	**100.0**	93.00	91.80	**100.0**
Mountain	69.00	85.78	82.85	82.43	72.25	84.00	42.00	**86.87**	68.20
Food	90.00	84.92	85.88	78.96	78.80	38.00	50.00	90.00	**99.40**
Average	84.70	86.85	86.10	84.21	80.57	78.30	69.70	90.15	**91.24**

Also, the precisions of the proposed CBIR scheme and methods reported in literature [18-25] in Corel-1k dataset are reported in Table 10. Here, the results were stated according to the highest 20 images [25]. It was noted that in these experiments, since 20 images are considered for precision and recal computation, these measures are increased sifnificantly in comparisaion with considering all images (Table 4).

From Table 6, the proposed method with precision 91.24% is the best method. On the other hand, the proposed method is the best method in 6 classes out of 10 classes.

4. 4. Retrieval Results　　　　A graphical comparison between all methods are performed in this secretion. For this task, a query image is considered as input for all methods and the retrieved output images of each method are depicted. Figures 9-15 show the retrieval results for flower query image in Corel-1k dataset. In these figures, the top left image (in orange box) is the query and the others are retrieved images. Images in blue box are similar to query and images in red box are irrelevant to query.

As shown in Table 11, the proposed method with precision 95.00% outperforms the other methods.

Figure 9. Retrieval results of the method in literature [11]

Figure 10. Retrieval results of the method in literature [8]

Figure 11. Retrieval results of the method in literature [10]

Figure 12. Retrieval results of the method in literature [12]

Figure 13. Retrieval results of the method in literature [13]

Figure 14. Retrieval results of the method in [15]

Figure 15. Retrieval results of the proposed method

TABLE 11. Conclusion of Figures 9-15

Method	$T = 20$		
	Number of similar images	Number of irrelevant images	Precision
[11]	7	13	35.00%
[8]	13	7	65.00%
[10]	18	2	90.00%
[12]	17	3	85.00%
[13]	18	2	90.00%
[15]	16	4	80.00%
Proposed	**19**	**1**	**95.00%**

Retrieval results of Figures 9-15 are concluded in Table 11.

4. 5. Computational Complexity   In this experiment, retrieval time of our CBIR system and CBIRs in literature [8, 10-13,15] are explored. Figure 16 reveals the comparison of the mean retrieval time in all CBIR systems applied to Corel-1k dataset. The proposed scheme is faster than methods in [12] and [15] and slower than the other methods.
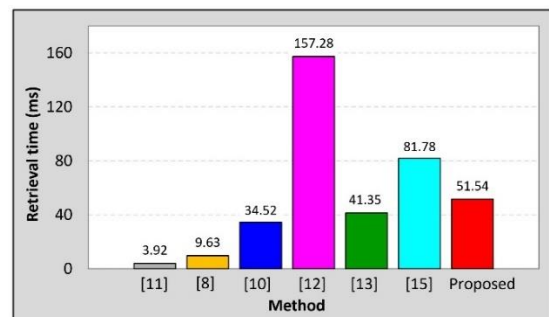

Figure 16. Retrieval time of the proposed method and literature [8, 10-13,15] in Corel-1k dataset

5. CONCLUSION

In this research, a new CBIR scheme was proposed. The proposed method focused on DCD features to improve

them. At first, the input image was transferred to gray-level image and then Canny edge detector was applied to image to determine image edges. In the next step, the morphological dilation was applied to edges to widen them. Finally, pixels that are located on the edges were assigned higher weight than the others. Corel-1k, Corel-10k and Caltech256 datasets were used for the evaluation and the experimental results indicated that the proposed CBIR method achieves better retrieval results in comparison with other competitive methods.

The limitation of the proposed DCD is that the SE size should be calculated for each dataset separately. For future work, precision of the proposed method can be checked on the different color spaces. Finally, determination of CBIR parameters using optimization algorithms such as particle swarm optimization (PSO) can be considered as another future work.

6. REFERENCES

1. Pavithra, L. K., and Sharmila, T. S., "Optimized feature integration and minimized search space in content based image retrieval", *Procedia Computer Science*, Vol. 165, (2019), 691-700, doi: 10.1016/j.procs.2020.01.065.

2. Fadaei, S., Amirfattahi, R., and Ahmadzadeh, M. R., "Local derivative radial patterns: A new texture descriptor for content-based image retrieval", *Signal Processing*, Vol. 137, (2017), 274-286, doi: 10.1016/j.sigpro.2017.02.013.

3. Dubey, S.R., Singh, S.K., and Singh, R.K., "Local neighbourhood-based robust colour occurrence descriptor for colour image retrieval", *IET Image Processing*, Vol. 9, No. 7, (2015), 578-586, doi: 10.1049/iet-ipr.2014.0769.

4. Singha, M., Hemachandran, K., and Paul, A., "Content-based image retrieval using the combination of the fast wavelet transformation and the colour histogram", *IET Image Processing*, Vol. 6, No. 9, (2012), 1221-1226, doi: 10.1049/iet-ipr.2011.0453

5. Pass, G. and Zabih, R., "Histogram refinement for content-based image retrieval", Proc. 3rd IEEE Workshop on Applications of Computer Vision (WACV'96), Sarasota, FL, (1996), 96-102, doi: 10.1109/ACV.1996.572008.

6. Chun, Y.D., Kim, N.C., and Jang, I.H., "Content-based image retrieval using multiresolution color and texture features", *IEEE Transactions on Multimedia*, Vol. 10, No. 6, (2008), 1073-1084, doi: 10.1109/TMM.2008.2001357.

7. Wang, X.-Y., Yu, Y.-J., and Yang, H.-Y., "An effective image retrieval scheme using color, texture and shape features", *Computer Standard Interfaces*, Vol. 33, No. 1, (2011), 59-68, doi: 10.1016/j.csi.2010.03.004.

8. Talib, A., Mahmuddin, M., Husni, H., and George, L. E., "A weighted dominant color descriptor for content-based image retrieval", *Journal of Visual Communication and Image Representation*, Vol. 24, No. 3, (2013), 345-360, doi: 10.1016/j.jvcir.2013.01.007.

9. Fadaei, S., Amirfattahi, R., and Ahmadzadeh, M. R., "New content-based image retrieval system based on optimised integration of DCD, wavelet and curvelet features", *IET Image Processing*, Vol. 11, No. 2, (2017), 89-98, doi: 10.1049/iet-ipr.2016.0542.

10. Deng, Y., Manjunath, B. S., Kenney, C., Moore, M. S., and Shin, H., "An efficient color representation for image retrieval", *IEEE Transactions on Image Processing*, Vol. 10, No. 1, (2001) 140-147, doi: 10.1109/83.892450.

11. Wang, X. Y., Yu, Y. J., and Yang, H. Y., "An effective image retrieval scheme using color, texture and shape features", *Computer Standards & Interfaces*, Vol. 33, No. 1, (2011), 59-68, doi: 10.1016/j.csi.2010.03.004.

12. Po, L. M., and Wong, K. M., "A new palette histogram similarity measure for MPEG-7 dominant color descriptor", In 2004 International Conference on Image Processing (ICIP'04), IEEE, (2004), 1533-1536, doi: 10.1109/ICIP.2004.1421357.

13. Mojsilovic, A., Kovacevic, J., Hu, J., Safranek, R. J., and Ganapathy, S. K., "Matching and retrieval based on the vocabulary and grammar of color patterns", *IEEE Transactions on Image Processing*, Vol. 9, No. 1, (2000), 38-54, doi: 10.1109/83.817597.

14. Fadaei, S., and Rashno, A., "Content-based image retrieval speedup based on optimized combination of wavelet and zernike features using particle swarm optimization algorithm", *International Journal of Engineering, Transactions B: Applications*, Vol. 33, No. 5, (2020), 1000-1009, doi: 10.5829/IJE.2020.33.05B.34.

15. Pavithra, L. K., and Sharmila, T. S., "An efficient seed points selection approach in dominant color descriptors (DCD)", *Cluster Computing*, Vol. 22, No. 4, (2019), 1225-1240, doi: 10.1007/s10586-019-02907-3.

16. Xie, G., Baolong, G., Zhe, H., Yan, Z., and Yunyi Y., "Combination of dominant color descriptor and Hu moments in consistent zone for content-based image retrieval", *IEEE Access*, Vol. 8, (2020), 146284-146299, doi: 10.1109/ACCESS.2020.3015285.

17. Sezavar, A., Farsi, H., and Mohamadzadeh, S., "A modified grasshopper optimization algorithm combined with cnn for content-based image retrieval", *International Journal of Engineering, Transactions A: Basics*, Vol. 32, No. 7, (2019), 924-930, DOI: 10.5829/IJE.2019.32.07A.04.

18. Irtaza, A., Adnan, S. M., Ahmed, K. T., Jaffar, A., Khan, A., Javed, A., and Mahmood, M. T., "An ensemble based evolutionary approach to the class imbalance problem with applications in CBIR", *Applied Sciences*, Vol. 8, No. 4, (2018), 495, doi: 10.3390/app8040495.

19. Mehmood, Z., Mahmood, T., and Javid, M. A., "Content-based image retrieval and semantic automatic image annotation based on the weighted average of triangular histograms using support vector machine", *Applied Intelligence*, Vol. 48, No. 1, (2018), 166-181, doi: 10.1007/s10489-017-0957-5.

20. Ali, N., Bajwa, K. B., Sablatnig, R., and Mehmood, Z., "Image retrieval by addition of spatial information based on histograms of triangular regions", *Computers & Electrical Engineering*, Vol. 54, (2016), 539-550, doi: 10.1016/j.compeleceng.2016.04.002.

21. Mehmood, Z., Anwar, S. M., Ali, N., Habib, H. A., and Rashid, M., "A novel image retrieval based on a combination of local and global histograms of visual words", *Mathematical Problems in Engineering*, (2016), doi: 10.1155/2016/8217250.

22. Zeng, S., Huang, R., Wang, H., and Kang, Z., "Image retrieval using spatiograms of colors quantized by gaussian mixture models", *Neurocomputing*, Vol. 171, (2016), 673-684, doi: 10.1016/j.neucom.2015.07.008.

23. Walia, E., and Pal, A., "Fusion framework for effective color image retrieval", *Journal of Visual Communication and Image Representation*, Vol. 25, No. 6, (2014), 1335-1348, doi: 10.1016/j.jvcir.2014.05.005.

24. Wang, C., Zhang, B., Qin, Z., and Xiong, J., "Spatial weighting for bag-of-features based image retrieval", In International Symposium on Integrated Uncertainty in Knowledge Modelling

and Decision Making, Springer, Berlin, Heidelberg, (2013), 91-100, doi: 10.1007/978-3-642-39515-4_8.

25. Alsmadi, M. K., "Content-based image retrieval using color, shape and texture descriptors and features", *Arabian Journal for Science and Engineering*, Vol. 45, No. 4, (2020), 3317-3330, doi: 10.1007/s13369-020-04384-y.

Persian Abstract

چکیده

بازیابی تصویر مبتنی بر محتوی یک فرایند برای بازیابی اتوماتیک تصاویر در یک پایگاه داده است. در حقیقت بازیابی تصویر مبتنی بر محتوی، یک راهحل برای جستجوی تصاویر مشابه با یک تصویر مطلوب (تصویر پرس وجو) در میان تمامی تصاویر پایگاه داده است. برای این منظور، روشهای متعددی برای استخراج ویژگیهای تصویر ارایه شده است. در این مقاله برای بهبود دقت بازیابی تصویر، یک روش جدید مبتنی بر ویژگیهای DCD ارایه شده است. در روش پیشنهادی، ابتدا تصویر رنگی به تصویر خاکستری تبدیل شده سپس لبههای تصویر به کمک لبهیاب کَنی آشکارسازی میشود. در مرحلهی بعد لبههای تصویر توسط عملیات مورفولوژی عریض میشوند. در نهایت در تشکیل ویژگیهای DCD، به پیکسلهایی که در مکان لبهها قرار دارند وزن بالاتری نسبت به دیگر پیکسلها داده میشود. در حقیقت، به پیکسلهایی که در نواحی با تغییرات روشنایی کم قرار دارند وزن کمتری اختصاص مییابد در حالیکه پیکسلهای با اطلاعات بالاتر وزن بیشتری خواهند داشت. به منظور ارزیابی روش پیشنهادی، نتایج پیادهسازی روی سه پایگاه دادهی Corel-1k، Coler-10k و Caltech256 ارایه شده است. نتایج نشان میدهند که روش پیشنهادی قابل رقابت با دیگر روشها است.